

⁹K. W. Mess, J. Lubbers, L. Nielsen, and W. J. Huiskamp, *Physica (Utrecht)* **41**, 260 (1969).

¹⁰Equation (3) assumes that the CMN is in thermal contact with a reservoir at constant temperature. We have observed this to be true under all the conditions of our experiment.

¹¹J. Bishop, thesis, University of California at San

Diego, 1973 (unpublished).

¹²J. P. Harrison and J. P. Pendry, *Phys. Rev. B* **8**, 5940 (1973).

¹³W. D. Halperin, C. N. Archie, F. B. Rasmussen, R. A. Buhrman, and R. C. Richardson, *Phys. Rev. Lett.* **32**, 927 (1974); J. M. Dundon and J. M. Goodkind, *Phys. Rev. Lett.* **32**, 1343 (1974).

Intense Focusing of Relativistic Electrons by Collapsing Hollow Beams

A. E. Blaugrund* and G. Cooperstein

Naval Research Laboratory, Washington, D. C. 20375

(Received 23 December 1974)

Low-impedance diodes with hollow tapered cathodes produce strong self-pinching in intense relativistic electron beams. Early in the pulse a thin hollow beam is formed, based on evidence of electrons striking the anode. This hollow beam collapses, accelerating toward the diode axis with velocities (1 to 5 mm/nsec) which depend locally on the anode material. An efficient and stable pinch, less than 3 mm in diameter, is formed at the anode. In the center 0.1 cm^2 , the power rises to 10^{11} W in less than 3 nsec. About 50% of the total diode energy ($\sim 9 \text{ kJ}$) is dissipated within the pinch region.

There has been considerable interest recently in intensely focused electron beams, primarily in connection with studies aimed at the achievement of pulsed fusion¹ in a manner analogous to that proposed using high-power lasers.² Typical electron-beam parameters considered necessary for pellet fusion are more than 10^{14} W of electrons of energies less than 3 MeV, efficiently delivered to a pellet approximately 3 mm in diameter in times less than 10 nsec.¹ In this Letter, we report on experiments with the U. S. Naval Research Laboratory's generator³ Gamble-I [750 keV, 500 kA, 70 nsec] which demonstrate efficient focusing of high-current relativistic electron beams to areas of about 0.1 cm^2 . Simultaneously, we have been able to overcome the limitations on current rise time posed by the Gamble-I generator (30 nsec), obtaining power rise times an order of magnitude shorter. Such rise-time limitations are quite general for high-power electron-beam accelerators.

Observations show that tapered hollow cathodes⁴ initially produce a thin hollow beam which collapses into a tight pinch at the anode center. In contrast to the pinch-formation process in plasma-channel diodes,⁵ negligible electron current strikes the center of the anode before the pinch is formed. The lack of early current near the anode center is responsible for the observed power rise time on axis of less than 3 nsec. More than 50% of the total diode energy is deposited in

the pinch region at a rate corresponding to 70% of the total diode power. Pinch currents and power densities in excess of $1.6 \times 10^6 \text{ A/cm}^2$ and 10^{12} W/cm^2 have been measured over areas of 0.1 cm^2 . Although similar current and power densities had been previously reported, the irradiated areas in these experiments are an order of magnitude larger.

The experiments described here were all done on the Gamble-I accelerator at total electron-beam energies of 8 to 9 kJ. A hollow cathode with an outer diameter of 84 mm and an inner diameter of 39 mm was used. The front face of the cathode was slightly tapered (at a 6° angle) with the anode-cathode spacing smallest at the inside edge. The majority of the shots were fired with a diode gap of 3.7 mm, giving a 3- Ω -impedance beam. In some shots, the impedance was reduced to about 2Ω by narrowing the gap. Figure 1(a) shows typical pulse forms of the diode current, voltage, and impedance. Note the flat plateau in the impedance curve which is characteristic of hollow cathodes operating in the self-pinch mode.⁶ The shot-to-shot reproducibility of these signals was about $\pm 3\%$. This diode never failed to produce a tight and reasonably well-centered pinch. Pinch locations all fell within a 3-mm radius around the diode axis as witnessed by damage patterns on the anode plates.

The spatial distribution of the current reaching the anode and its time behavior were investigated

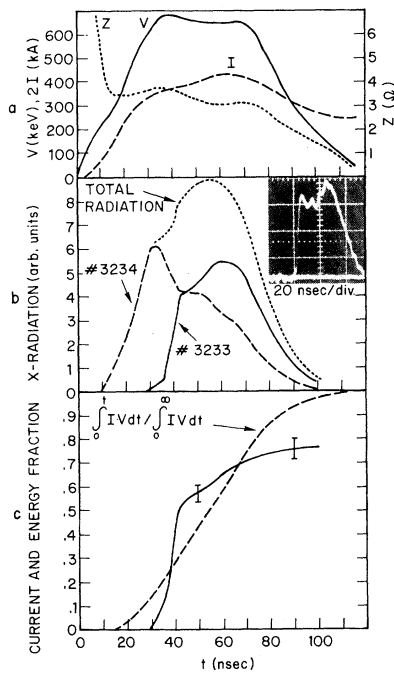


FIG. 1. (a) Typical diode voltage (V), current (I), and impedance (Z). The voltage has been corrected for inductive contributions. (b) Measured x radiation from both inside (No. 3233) and outside (No. 3234) an 11-mm-diam central region of the anode. The curve labeled "total radiation" is the computed sum of the two signals. The inset shows the fast-rising radiation pulse observed with a smaller aperture and a well-centered pinch. (c) Fraction of total diode current versus time contained within the central 11-mm-diam region of the anode (solid curve). The error bars indicate the typical spread in these data. The dashed curve gives the fraction of total beam energy dissipated up to a time t . The total beam energy was 8.7 kJ.

by means of a number of fast photodiode-scintillator detectors looking at the bremsstrahlung radiation from selected parts of the anode through various thicknesses of x-ray absorbers. By comparing the detector signals obtained with different sets of collimators, it was possible to determine the current distribution between the various anode regions at any time within the pulse. Figure 1(b) shows an example of signals recorded with unshielded scintillation detectors looking at the anode through collimators. In shot No. 3233, only radiation from the central region (11 mm in diameter) was recorded. In shot No. 3234, radiation from the entire anode with the exception of the central region was measured. The curve labeled "total radiation" is the computed sum of the two signals. It can be seen that although radi-

ation is observed very early in the pulse, practically none of it comes from the central region of the anode during the first 30 nsec. When the radiation finally appears at the center, it rises rapidly with a rise time ≈ 5 nsec and persists for the remainder of the pulse. The small precursor which appears in this figure is due to a small eccentricity of the pinch. It is absent in well-centered pinches where scope-limited rise times (≤ 3 nsec) are observed [see inset in Fig. 1(b)].

From these two signals, the fraction of the electron-beam current hitting the center region can be deduced. Figure 1(c) shows this fraction as a function of time. The curve represents the average of data obtained with detectors looking through x-ray absorbers of various thicknesses. All these detectors gave essentially the same results and the error bars in Fig. 1(c) represent the spread between them. This agreement between detectors recording different parts of the x-ray spectrum indicates that, at any time during the pulse, the kinetic energy was the same for electrons hitting the anode either inside or outside the pinch region. Thus, the use of the relative bremsstrahlung yield for determining the electron-current distribution is justified. It can be seen from Fig. 1(c) that as the beam pinches, the fraction of the current reaching the center 11-mm-diam region rises rapidly from practically zero to about 50% of the total diode current, and then increases slowly to about 75%. Similar behavior was observed with a 2- Ω diode except that the initial and final fractions were 65 and 80%, respectively. Other data show that, after pinch formation, more than 90% of the electrons strike the anode within an area opposite the cathode recess. Also included in Fig. 1(c) is a curve showing the fraction of total beam energy deposited on the entire anode up to time t . It can be deduced from the two curves in Fig. 1(c) that about 50% of the total beam energy is deposited in the pinch region.

X-ray pinhole photographs were taken with pinhole diameters of 0.2 and 0.3 mm. These photographs showed an intense rather flat-topped spot at the center of the anode and densitometer scans reproducibly gave spot diameters of 3 mm (full width at half-maximum). With use of the film-density profile and the beam current in the pinch region as determined above, a peak current density in the pinch of 1.6×10^6 A/cm² was estimated.

In another experiment, a 1-mm-thick aluminum anode plate was covered on the outside with a 0.5-mm-thick Pilot-B scintillator. The anode

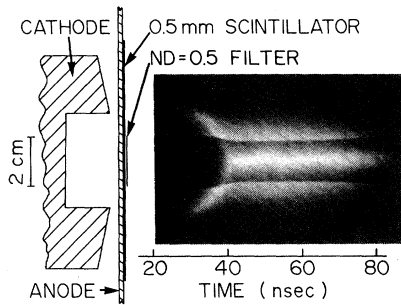


FIG. 2. Streak photograph of scintillator along anode diameter. Zero time coincides with the start of the voltage pulse (see Fig. 1). Light from the central part has been attenuated by a neutral-density filter. The size of the filter varies on the photograph because of distortions in the image-converter tube.

plate was thick enough to stop the electrons so that the light in the scintillator was generated by the transmitted bremsstrahlung. The face of the scintillator was photographed with TRW model-1D image-converter cameras. Both framing (5-nsec exposure) and streak photographs (~ 2 -nsec resolution) were obtained. Figure 2 shows a drawing of the experimental arrangement together with a streak photograph of a scintillator. In order to bring the widely varying light intensities within the limited dynamic range of the camera, the central portion of the scintillator was covered by an optical neutral-density filter. The photograph shows a thin (< 3 mm) hollow shell of electrons forming at a radius slightly larger than the cathode inner radius. The shell collapses toward the center, continuously accelerating. The initial collapse velocity is ~ 0.8 mm/nsec. Average velocities for radii between 10 and 15 mm and for radii less than 10 mm are 1.7 and 3.6 mm/nsec, respectively. By about 40 nsec after the beginning of the pulse, the shell has collapsed into a tight pinch at the center of the anode. The pinch persists for the remaining 50 nsec making erratic excursions of ~ 1 mm about the diode axis. This movement may account for a part of the 3-mm pinch diameter measured in time-integrated x-ray pinhole exposures. The pinch diameter deduced from the image-converter pictures is less than 3 mm (the spatial resolution of the anode-scintillator combination). Therefore, the actual pinch diameter may be smaller and the peak current densities prevailing within the pinch may be much higher than 10^6 A/cm². Framing pictures taken during the beam collapse time showed circular symmetric shells.

In similar experiments with brass anodes, the beam shell collapsed with an initial velocity of ~ 1.4 mm/nsec rising to an average velocity of 4.4 mm/nsec in the last 10 mm of travel. In these cases, a tight pinch is formed about 12 nsec earlier than in cases using an aluminum anode and appears to be somewhat less stable. Experiments with brass anodes coated with very thin (~ 1 μ m) layers of aluminum show that the collapse velocity is determined by the surface layer. Composite anodes made of a center aluminum disc in a brass anode exhibit a collapse velocity which depends locally on the type of material being struck by the imploding electron ring. Simple calculations indicate that the energy deposited in the metal by the moving electron ring is not sufficient to vaporize the bulk of the material. It has been suggested⁷ that low-density ions emanating from the anode surface affect the flow of electrons in the diode and that the collapse velocity depends on the production rate and velocity of these ions. At this stage it is not clear whether ions of the metal or of absorbed gasses are responsible for this process.

Preliminary results obtained with the more powerful Gamble-II accelerator⁸ indicate that the phenomena remain essentially unchanged at 4 times greater total beam energy. Higher collapse velocities and higher current and power densities have been observed while the pinch diameter remained the same.

The discovery of the thin hollow collapsing electron beam makes possible the realization of experiments and techniques requiring fast-rising electron pulses which otherwise would have required fast-rise-time accelerators not yet available with present-day technology. Future progress depends on improving our understanding of the basic physical mechanisms involved. No satisfactory analytical or computational time-dependent model describing the pinch phenomenon has been published to date. The detailed phenomenological description of the diode behavior given here may facilitate the construction of such models. Further experimental and theoretical⁷ work is presently in progress.

The authors would like to thank J. R. Boller and J. J. Condon for experimental assistance and D. Mosher for helpful suggestions and criticisms.

*On leave of absence from the Weizmann Institute of Science, Rehovot, Israel.

[†]G. Yonas, J. W. Poukey, K. R. Prestwich, J. R.

Freeman, A. J. Toepfer, and M. J. Clauser, to be published; L. I. Rudakov and A. A. Samarsky, in *Proceedings of the Sixth European Conference on Controlled Fusion and Plasma Physics, Moscow, U. S. S. R., 1973* (U.S.S.R. Academy of Sciences, Moscow, 1973), p. 487.

²J. Nuckolls, L. Wood, A. Thiessen, and G. Zimmerman, *Nature* **239**, 139 (1972); K. A. Brueckner and S. Jorna, *Rev. Mod. Phys.* **46**, 325 (1974).

³G. Cooperstein, J. J. Condon, and J. R. Boller, *J. Vac. Sci. Technol.* **10**, 961 (1973).

⁴G. Cooperstein, J. G. Siambis, and J. J. Condon, *Bull. Amer. Phys. Soc.* **19**, 532 (1974).

⁵G. Yonas, K. R. Prestwich, J. W. Poukey, and J. R. Freeman, *Phys. Rev. Lett.* **30**, 164 (1973); P. A. Miller, J. Chang, and G. W. Kuswa, *Appl. Phys. Lett.* **23**, 423 (1973); K. M. Glibert, J. Chang, and L. P. Mix, *Bull. Amer. Phys. Soc.* **19**, 869 (1974).

⁶G. Cooperstein, J. J. Condon, and J. R. Boller, *Bull. Amer. Phys. Soc.* **18**, 1310 (1973); G. Cooperstein and J. J. Condon, to be published.

⁷S. A. Goldstein and J. G. Siambis, private communication.

⁸L. S. Levine and I. M. Vitkovitsky, *IEEE Trans. Nucl. Sci.* **18**, No. 4, 225 (1971).

Measurement of Ion-Acoustic Plasma Turbulence by Cross-Power Spectra*

Dragan B. Ilić,

Institute for Plasma Research, Stanford University, Stanford, California 94305

(Received 21 October 1974)

The propagation of current-driven ion-acoustic waves in a positive column is studied by measuring the cross-power spectral density up to 30 MHz. Dispersion characteristics are verified in the weakly turbulent state, and the measurements of instability correlation times and lengths are illustrated for higher levels of turbulence, where the dispersion relation no longer applies.

Statistical methods are very useful for analyzing the results of experiments in weakly turbulent plasmas, where many interacting waves are present: The cross-correlation function is used in the time domain, while its Fourier transform, the cross-power spectral density, is used in the frequency domain.¹ The currently available cross correlators can process signals of at most a few megahertz,^{1,2} unless sampling techniques are used,³ while the application of well-developed signal-processing techniques in the frequency domain⁴ can, in principle, lead to analog instruments for measuring the cross-power spectra in the gigahertz range.²

This note reports the results of studying ion-acoustic waves in a weakly turbulent plasma, obtained by measuring the cross-power spectral density up to 30 MHz. While measurements of the cross-power spectra below 1 MHz have been used to deduce the ambipolar diffusion coefficient⁵ and electron density⁶ in thermal plasmas, and the spectral index in turbulent plasmas,⁷ we believe this to be the first application of the cross-power spectra to the study of propagating plasma waves up to 30 MHz. It will be demonstrated that important information about the turbulent characteristics of saturated instabilities can be obtained in this way.

For a given pressure, current-driven ion-

acoustic waves are excited in the positive column above a critical value of discharge current, in the form of a band of frequencies around the frequency f_0 for which the convective growth rate

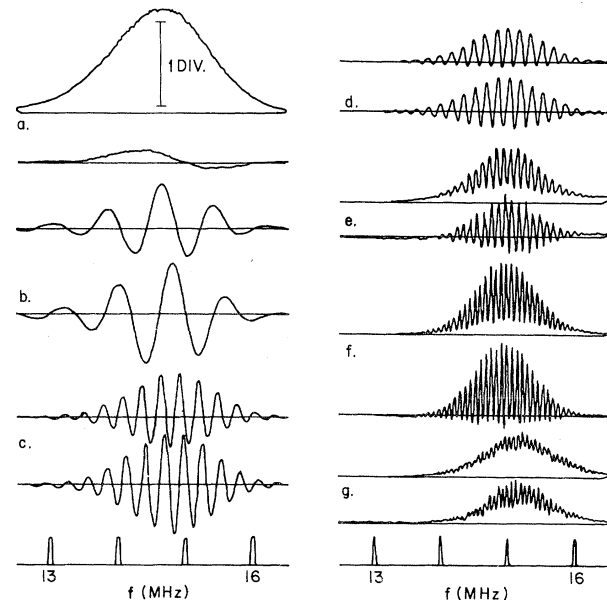


FIG. 1. The cross-power spectra at $pa=0.48$ Torr cm, $I=2.5$ A, and the following probe separations Δz (mm), and vertical sensitivities (mV/div): (a) 0, 20; (b) 10, 50; (c) 30, 50; (d) 50, 50; (e) 80, 10; (f) 110, 20; (g) 130, 10.

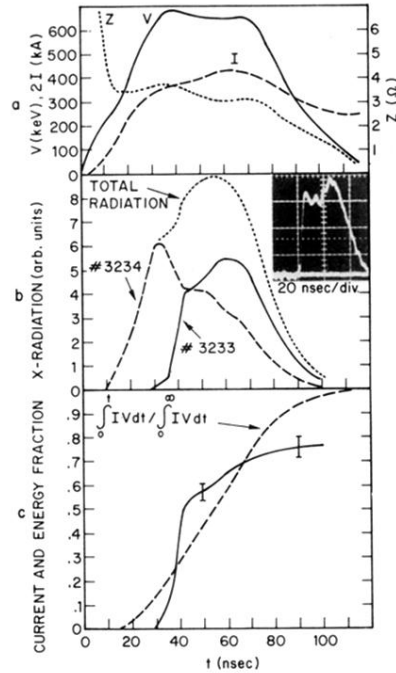


FIG. 1. (a) Typical diode voltage (V), current (I), and impedance (Z). The voltage has been corrected for inductive contributions. (b) Measured x radiation from both inside (No. 3233) and outside (No. 3234) an 11-mm-diam central region of the anode. The curve labeled "total radiation" is the computed sum of the two signals. The inset shows the fast-rising radiation pulse observed with a smaller aperture and a well-centered pinch. (c) Fraction of total diode current versus time contained within the central 11-mm-diam region of the anode (solid curve). The error bars indicate the typical spread in these data. The dashed curve gives the fraction of total beam energy dissipated up to a time t . The total beam energy was 8.7 kJ.

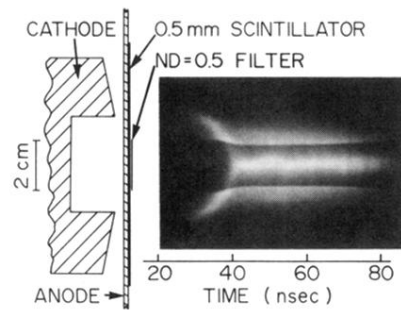


FIG. 2. Streak photograph of scintillator along anode diameter. Zero time coincides with the start of the voltage pulse (see Fig. 1). Light from the central part has been attenuated by a neutral-density filter. The size of the filter varies on the photograph because of distortions in the image-converter tube.